

Model Prediction-Based Approach to Fault Tolerant Control with Applications

Magdi S. Mahmoud and Haris M. Khalid

Abstract—Fault-tolerant control (FTC) is an integral component in industrial processes as it enables the system to continue robust operation under some conditions. In this paper, an FTC scheme is proposed for interconnected systems within an integrated design framework to yield a timely monitoring and detection of fault and reconfiguring the controller according to those faults. The unscented Kalman filter (UKF)-based fault detection and diagnosis system is initially run on the main plant and parameter estimation is being done for the local faults. This critical information is shared through information fusion to the main system where the whole system is being decentralized using the overlapping decomposition technique. Using this parameter estimates of decentralized subsystems, a model predictive control (MPC) adjusts its parameters according to the fault scenarios thereby striving to maintain the stability of the system. Experimental results on interconnected continuous time stirred tank reactors (CSTR) with recycle and quadruple tank system indicate that the proposed method is capable to correctly identify various faults, and then controlling the system under some conditions.

Index Terms—Fault tolerant control; Unscented Kalman filter; Decentralized control; Overlapping decomposition; Model predictive control, CSTR units, Quadruple tank system.

NOMENCLATURE

The variables used throughout the paper are expressed in Table I. Moreover, $f(\cdot)$, $g(\cdot)$ and $h(\cdot)$ are also added in the nomenclature.

I. INTRODUCTION

IN process control industry, failures of some key control and process elements are often encountered. The failure of such major components will not only effect the performance of the plant, but it will lead to critical operation problems leading to instability and possible breakdown. For example, a faulty sensor may easily effect the momentum of the production line and in some cases may push the other sensors in the plant to work beyond their design configuration, thereby leading to a major control failure in the sensor network-based monitoring of the plant. Other crucial scenarios can be a burned-out thermocouple, a broken transducer or a stuck valve. Therefore, fault tolerance has been one of the major issues in process control, and its high availability has become a basic component for the process industries.

Fault-tolerance or graceful degradation is basically the design property that enables the system to continue operation under some conditions, when some part of the system fails. Because of the poor health of the system, the operation continues certainly at a reduced level, rather than failing completely. Moreover, the performance is proportional to the severity of the failure, as compared to a conventionally-designed system

Manuscript MsM-KFUPM-Haris-FTC-1.tex

M. S. Mahmoud is with the Systems Engineering Department, King Fahd University of Petroleum and Minerals, P. O. Box 985, Dhahran 31261, Saudi Arabia, e-mail: msmahmoud@kfupm.edu.sa.

H. M. Khalid is with the Systems Engineering Department, King Fahd University of Petroleum and Minerals, P. O. Box 5067, Dhahran 31261, Saudi Arabia, e-mail: mhariskh@kfupm.edu.sa

TABLE I
NOMENCLATURE

Symbols	Function
\bar{x}	Mean
P_x	Covariance
$2L + 1$	Sigma vectors in UKF
QTS	Quadruple tank System
UT	Unscented transformation
α	Spread of the sigma points around \bar{x}
κ	Secondary scaling parameter
β	Incorporate prior knowledge of x distrb.
λ	Composite scaling parameter
L	Dimension of the augmented state
R^v	Process-noise covariance
R^n	Measurement-noise covariance
W_i	Weights
w_k	Identity state transition matrix
r_k	Noise
d_k	Desired output
w_k	Nonlinear observation
R^e	Constant diagonal matrix
λ_{RLS}	Forgetting factor
h_i	Level of water in tank i in QTS
a_i	Area of water flowing out from tank i in QTS
A_i	Area of tank i
γ_1	QTS: tank 1 and tank 4 water diverting ration
γ_2	QTS: tank 2 and tank 3 water diverting ration
k_1	Gain of Pump 1 in QTS
k_2	Gain of Pump 2 in QTS
ν_1	QTS: Manipulated input 1 (pump 1)
ν_2	QTS: Manipulated input 2 (pump 2)
g	Gravitational constant in QTS
a_{leaki}	QTS: Leak in pipe of tank i in QTS
q_{in}	Inflow in QTS
q_{out}	Outflow in QTS
A	Reactant species
B	Desired product
U, R	Undesired byproducts
T_j	Reactor temp.
C_{Aj}	Concentration of A
Q_j	Reactor heat input rate
V_j	Reactor volume
c_p	Heat capacity
ρ	Fluid density in reactor
$f(\cdot), g(\cdot), h(\cdot)$	Non-linear functions

in which even a small failure can cause total breakdown. The problem of fault tolerance is of extreme importance when it comes to mission critical systems and life-critical systems and several approaches have been adopted to implement a reliable fault tolerant control scheme. Result on FTC for a direct-drive wind turbines and five-phase permanent-magnet motors are reported in [1] and [2], respectively. A scheme for optimal torque FTC is proposed in [3]. A work on multi-phase power converter drive for fault-tolerant machine development in aerospace application is presented in [4]. Recent FTC applications are found in [5], [6]. Depending upon how the redundancy is being utilized, FTC system design can be classified into two types:

- Passive fault tolerant control (PFTC) systems, and
- Active fault tolerant control (AFTC) systems.

In PFTC systems, controllers are fixed and are designed to be robust against a class of *a priori* known faults. This approach needs neither fault diagnosis and detection (FDD) schemes nor controller reconfiguration, but it has limited fault-tolerant capabilities. Once the controller is designed in the passive fault tolerant scheme, it will remain fix during the entire system operation. Even in the event of component failures, the control system should be able to maintain the designed performance. A multiple disjoint decentralized control was proposed, in which redundancy lies in the employment of multiple controllers [7]. Further extensions to control design against actuator failures was developed using a state-feedback controller implementation [8]-[9]. PFTC is also known in the literature as reliable control systems or control systems with integrity.

In contrast to PFTC system, AFTC systems react to component failures actively by reconfiguring control actions so that the stability and acceptable performance of the entire system can be maintained. AFTC system is also referred to as self-repairing [11], reconfigurable [12], restructurable [14], or self-designing [15] systems. AFTC system consists basically of a) a fault detection and diagnosis scheme b) controller reconfiguration mechanism, and c) reconfigurable controller, with all of these ingredients have to work in a systematic manner. In this regard, AFTC systems were also named as fault detection, identification (diagnosis) and accommodation schemes [16]-[17]. Also [25] presents a strong tracking filter based generic model control which leads to the reconfigurable controllers. Work on AFTC for magnetic levitation systems is being made in [26]-[27], where sensor faults have been considered.

In this paper, we have proposed an AFTC system. An improved FTC scheme is developed within an integrated fault detection and tolerance-based design framework. The developed methodology utilizes a model-prediction based fault tolerant technique to enhance the accuracy and reliability of parametric estimation done through UKF in the process fault detection phase. The main contribution of the paper is the incorporation of the model-prediction based fault control at the later stage, handling the system, with the UKF based improved fault detection and estimation at the former stage. The proposed scheme has then been successfully evaluated on an interconnected CSTR unit with recycle and quadruple tank systems, thus corroborating the theory underpinning it.

The paper is organized as follows: Fault tolerant problem

statement and the proposed solution formulation is presented in section II, followed by the evaluation of the proposed scheme in section III. Section IV presents the simulation results for the techniques implemented. Finally some concluding remarks are given in section V.

II. SYSTEM DESCRIPTION

To have an effective fault detection and tolerance, we have assumed various faults in an interconnected system have been successfully monitored, estimated and protected through tolerance by the encapsulation of the UKF with model-prediction based decentralized control. Fig. 1 shows the proposed implementation plan. Unscented filters are employed in n states of the system. They are planted here for the fault detection purpose in high dynamic system. The residual is comparing the output of unscented filters' output and output of n states of a healthy model of the plant which contain no faults, this results in n residuals r_n , which will give us the drift detection of the system, these drift detections and output of the unscented filters will add in a summer to give us the parameter estimation of the system. The drift detection and parameter estimation are fed in an information unit known as FDD unit, from where the information is fused, and proceeds further to the subsystems of a particular system, made by overlapping decomposition, the fused information tells the potency of the fault and its upper and lower limits, which helps us to build a decentralized MPC-based fault tolerant controller, which adjusts its parameters according to the fault scenarios thereby striving to maintain the stability of the system.

Assume that a process is monitored by N different sensors, described by the following general nonlinear process and measurement models in discrete time state-space framework:

$$\begin{aligned} x(k) &= f(x(k-1), u(k-1), d(k-1)) + w(k-1) \\ z_i(k) &= c_i(x(k)) + \nu_i(k); \quad i = 1, \dots, N \end{aligned} \quad (1)$$

where $f(\cdot)$ and $h_i(\cdot)$ are the known nonlinear functions, representing the state transition model and the measurement model, respectively. $x(k) \in R_{n_x}$ is the process state-vector, $u(k) \in R_{n_u}$ denotes the manipulated process variables, $d(k) \in R_{n_d}$ represents the process faults modeled by the process disturbances, $z_i(k) \in R_{n_{z_i}}$ are the measured variables obtained from the N installed sensors, $w(k)$ and $v_i(k)$ indicate the stochastic process and measurement disturbances modeled by zero-mean white Gaussian noises with covariance matrices $Q(k)$ and $R_i(k)$, respectively.

A. Discrete-time UKF

In most practical applications of interest, the process and/or measurement dynamic models are described by non-linear equations, represented in system (1). This means that the non-linear behavior can affect the process operation at least through its own process dynamics or measurement equation. In such cases, the standard Kalman filter algorithm is often unsuitable to estimate the process states using its linearized time-invariant state-space model at the desired process nominal operating point. UKF gives a simple and effective remedy to overcome such non-linear estimation problem. Its basic idea is to

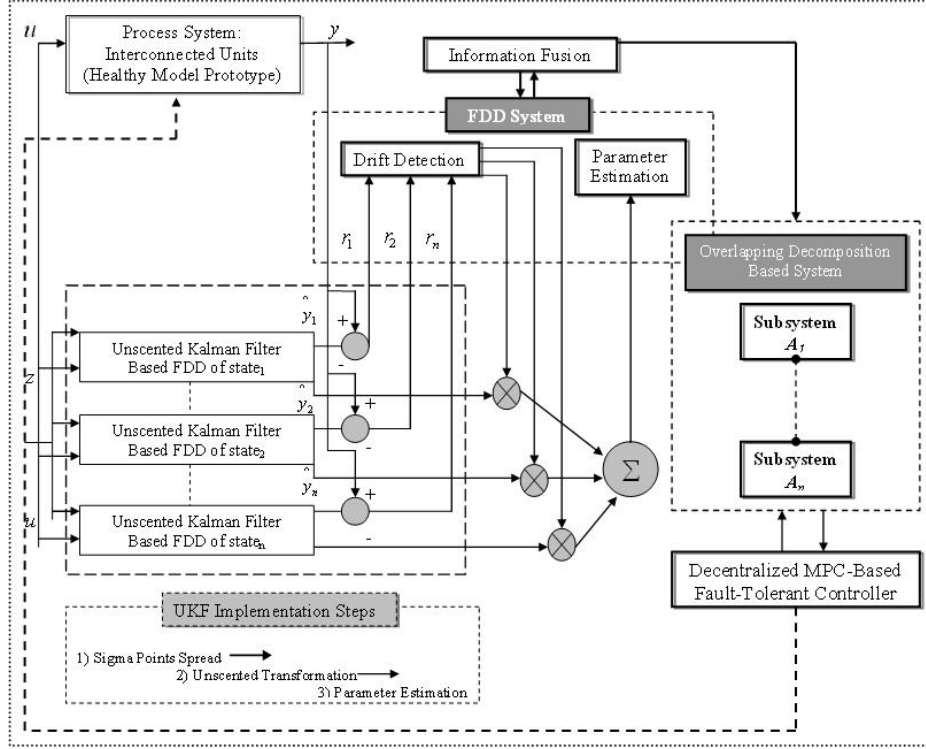


Fig. 1. FTC implementation plan

locally linearize the non-linear functions, described by system (1), at each sampling time instant around the most recent process condition estimate. This allows the Kalman filter to be applied to the following linearized time varying model:

$$\begin{aligned} x(k) &= A(k)x(k-1) + B_u(k)u(k-1) + B_d(k)d(k-1) \\ &\quad + w(k-1) \\ z_i(k) &= C_i(k)x(k) + \nu_i(k); \quad i = 1, \dots, N \end{aligned} \quad (2)$$

where the state transition matrix $A(k)$, the input matrices $B_u(k)$ and $B_d(k)$, and the observation matrix $H_i(k)$ are the jacobian matrices which are evaluated at the most recent process operating condition in real-time rather than the process fixed nominal values:

$$A(k) = \frac{\partial f}{\partial x} \Big|_{\hat{x}(k)}, \quad B_u(k) = \frac{\partial f}{\partial u} \Big|_{u(k)} \quad (3)$$

$$B_d(k) = \frac{\partial f}{\partial d} \Big|_{d(k)}, \quad C_i(k) = \frac{\partial h_i}{\partial x} \Big|_{\hat{x}(k)}, \quad i = 1, \dots, 10 \quad (4)$$

In conventional control, disturbance variables $d(k)$ are treated as known inputs with distinct entry in the process state-space model. This distinction between state and disturbance as non-manipulated variables, however, is not justified from the monitoring perspective using the estimation procedure. Therefore, a new augmented state variable vector $x^*(k) = [d^T(k) \quad x^T(k)]^T$ is developed by considering the process disturbances or faults as additional state variables. To implement

this view, the process faults are assumed to be random state variables governed by the following stochastic auto-regressive (AR) model equation:

$$d(k) = d(k-1) + w_d(k-1) \quad (5)$$

This assumption changes the linearized model formulations in system (2) to the following augmented state-space model:

$$\begin{aligned} x^*(k) &= A^*(k)x^*(k-1) + B^*(k)u(k-1) + \\ &\quad w^*(k-1) \\ z_i(k) &= C_i^*(k)x^*(k) + \nu_i(k); \quad i = 1, \dots, N \end{aligned} \quad (6)$$

Noting that:

$$\begin{aligned} A^*(k) &= \begin{bmatrix} I^{n_d \times n_d} & 0^{n_d \times n_x} \\ B_d(k)^{n_x \times n_d} & A(k)^{n_x \times n_x} \end{bmatrix} \\ B^*(k) &= [0^{n_d \times n_u} \quad B_u(k)^{n_x \times n_u}]^T \\ C_i^*(k) &= [0^{1 \times n_d} \quad C_i(k)^{1 \times n_x}] \\ W^*(k-1) &= [w_d(k-1)^{n_d \times 1} \quad w(k-1)^{n_x \times 1}]^T \end{aligned} \quad (7)$$

Assumption II.1: There exists a known positive constant L_0 such that for any norm bounded $x_1(t), x_2(t) \in \mathbf{R}^n$, the following inequality holds:

$$\begin{aligned} &\|f(u(t), y(t), x_1(t)) - f(u(t), y(t), x_2(t))\| \\ &\leq L_0 \|x_1(t) - x_2(t)\| \end{aligned} \quad (8)$$

Assumption II.2: The transfer function matrix $C[zI - (A - KC)]^{-1}B$ is strictly positive real, where $K \in \mathbf{R}^{n \times r}$ is chosen such that $A - KC$ is stable.

Remark II.1: For a given positive definite matrix $Q > 0 \in \mathbf{R}^{n \times n}$, there exists matrices $P = P^T > 0 \in \mathbf{R}^{n \times n}$ and a scalar R such that:

$$(A - KC)^T P (A - KC) = -Q \quad (9)$$

$$PB = C^T R \quad (10)$$

To detect the fault, the following is constructed:

$$\begin{aligned} \hat{x}(k) &= A\hat{x}(k) + g(u(k), y(k)) + B\xi_H f(u(k), y(k), \hat{x}(k)) \\ &\quad + K(y(k) - \hat{y}(k)) \end{aligned} \quad (11)$$

$$\hat{y}(k) = C\hat{x}(k) \quad (12)$$

where $\hat{x}(k) \in \mathbf{R}^n$ is the state estimate, the input is $u \in \mathbf{R}^m$, and the output is $y \in \mathbf{R}^r$. The pair (A, C) is observable. The non-linear term $g(u(k), y(k))$ depends on $u(k)$ and $y(k)$ which are directly available. The $f(u(k), y(k), x(k)) \in \mathbf{R}^r$ is a non-linear vector function of $u(k)$, $y(k)$ and $x(k)$. The $\xi(k) \in \mathbf{R}$ is a parameter which changes unexpectedly when a fault occurs. Since it has been assumed that the pair (A, C) is observable, a gain matrix K can be selected such that $A - KC$ is a stable matrix. We define:

$$e_x(k) = x(k) - \hat{x}(k), \quad e_y(k) = y(k) - \hat{y}(k) \quad (13)$$

Then, the error equations can be given by:

$$\begin{aligned} e_x(k+1) &= (A - KC)e_x(k) + B[\xi(k)f(u(k), y(k), x(k)) \\ &\quad - \xi_H f(u(k), y(k), \hat{x}(k))], \end{aligned} \quad (14)$$

$$e_y(k) = Ce_x(k) \quad (15)$$

The convergence of the above filter is guaranteed by the following theorem II.1:

Theorem II.1: Under the assumption (II.2), the filter is asymptotically convergent when no fault occurs ($\xi(k) = \xi_H$), i.e. $\lim_{k \rightarrow \infty} e_y(k) = 0$.

Proof: Consider the following Lyapunov function

$$V(e(k)) = e_x^T(k) P e_x(k) \quad (16)$$

where P is the solution of (9), Q is chosen such that $\rho_1 = \lambda_{\min}(Q) - 2\|C\| \cdot \|R\| \xi_H L_0 > 0$. Along the trajectory of the fault-free system (14), the corresponding Lyapunov difference along the trajectories $e(k)$ is:

$$\begin{aligned} \Delta V &= E\{V(e(k+1)|e_k, p_k)\} - V(e(k)) \\ &= E\{e^T(k+1)P_i e(k+1)\} - e^T(k)P_i e(k) \\ &= (A_e e_x + B_L u_e)^T P (A_e e_x + B_L u_e) - e_x^T(k) P e_x(k) \\ &= e^T(k) [(P(A - KC) + (A - KC)^T P) \\ &\quad + PB\xi_H [f(u(k), y(k), x(k)) \\ &\quad - f(u(k), y(k), \hat{x}(k))]] e(k) \end{aligned} \quad (17)$$

From (II.1) and system (9), one can further obtain that

$$\begin{aligned} \Delta V &\leq -e_x^T(k) Q e_x(k) + 2\|e_y(k)\| \cdot \|R\| \xi_H L_0 \|e_x(k)\| \\ &\leq -\rho_1 \|e_x\|^2 < 0 \end{aligned} \quad (18)$$

Thus, $\lim_{k \rightarrow \infty} e_x(k) = 0$ and $\lim_{k \rightarrow \infty} e_y(k) = 0$. This completes the proof. ■

The UKF essentially addresses the approximation issues of the EKF [18], [19], [20]. The basic difference between the EKF and UKF stems from the manner in which Gaussian random variables (GRV) is presented through system dynamics. In the EKF, the state distribution is approximated by GRV, which is then propagated analytically through the first-order linearization of the non-linear system. This can introduce large errors in the true posterior mean covariance of the transformed GRV, which may lead to sub-optimal performance and sometimes divergence of the filter. The UKF addresses this problem by using a deterministic sampling approach. The state distribution is again approximated by a GRV, but is now represented using a minimal set of carefully chosen sample points. These sample points completely capture the true mean and covariance of the GRV, and when propagated through the *true* non-linear system, capture the posterior mean and covariance accurately to second order (Taylor Series Expansion) for any nonlinearity. The EKF, in contrast, only achieves first-order accuracy.

A.1 Unscented Transformation (UT)

The structure of the UKF is elaborated by UT for calculating the statistics of a random variable which undergoes a nonlinear transformation [20]. Consider propagating a random variable \mathbf{x} (dimension L) through a nonlinear function, $y = f(x)$. Assume \mathbf{x} has mean \bar{x} and covariance P_x . To calculate the statistics of y , we form a matrix \mathcal{X} of $2L + 1$ sigma vectors \mathcal{X}_i according to:

$$\begin{aligned} \mathcal{X}_0 &= \bar{x}, \\ \mathcal{X}_i &= \bar{x} + (\sqrt{(L + \lambda)P_x})_i, \quad i = 1, \dots, L \\ \mathcal{X}_i &= \bar{x} - (\sqrt{(L + \lambda)P_x})_i - L, \quad i = L + 1, \dots, 2L \end{aligned} \quad (19)$$

where $\lambda = \alpha^2(L + \kappa) - L$ is a scaling parameter. The constant α determines the spread of the sigma points around \bar{x} , and is usually set to a small positive value ($1 \leq \alpha \leq 10^{-4}$). The constant κ is a secondary scaling parameter, which is usually set to $3 - L$, and β is used to incorporate prior knowledge of the distribution of \mathbf{x} (for Gaussian distributions, $\beta = 2$) is optimal). $(\sqrt{(L + \lambda)P_x})_i$ is the i th column of the matrix square root (that is, lower-triangular Cholesky factorization). These sigma vectors are propagated through the nonlinear function $\mathcal{Y}_i = f(\mathcal{X}_i), i = 0, \dots, 2L$. Now the mean and covariance for y are approximated using a weighted sample mean and covariance of the posterior sigma points:

$$\begin{aligned} \bar{y} &\approx \sum_{i=0}^{2L} W_i^m \mathcal{Y}_i, \\ P_y &\approx \sum_{i=0}^{2L} W_i^c (\mathcal{Y}_i - \bar{y})(\mathcal{Y}_i - \bar{y})^T, \\ W_0^{(m)} &= \frac{\lambda}{L + \lambda}, \\ W_0^{(c)} &= \frac{\lambda}{L + \lambda} + 1 - \alpha^2 + \beta, \\ W_i^{(m)} &= W_i^{(c)} = \frac{1}{2(L + \lambda)}, i = 1, \dots, 2L. \end{aligned}$$

A block diagram illustrating the steps in performing the UT is shown in Fig. 1.

Remark II.2: Note that this method differs substantially from general Monte Carlo sampling methods which require orders of magnitude more sample points in an attempt to propagate an accurate (possibly non-Gaussian) distribution of the state. The deceptively simple approach taken with the UT results in approximations that are accurate to the third order for Gaussian inputs for all nonlinearities. For non-Gaussian inputs, approximations are accurate to at least the second order, with the accuracy of the third- and higher order moments being determined by the choice of α and β .

A.2 Extension to UT: The UKF

In view of the foregoing, the UKF is an extension of the UT to the following recursive estimation:

$$\hat{x}_k = x_{k_{prediction}} + \kappa_k [y_k - y_{k_{prediction}}] \quad (20)$$

where the state random variables (RV) is redefined as the concentration of the original state and noise variables: $x_k^a = [x_k^T \ v_k^T \ n_k^T]^T$. The UT sigma point selection scheme is then applied to this new augmented state RV to calculate the corresponding sigma matrix, \mathcal{X}_k^a . The UKF equations are given below. Note that no explicit calculations of Jacobian or Hessians are necessary to implement this algorithm. Initialize with 21:

$$\begin{aligned} \hat{x}_0 &= \mathbf{E}[x_0], \\ P_0 &= \mathbf{E}[(x_0 - \hat{x}_0)(x_0 - \hat{x}_0)^T], \\ \hat{x}_0^a &= \mathbf{E}[x^a] = [\hat{x}_0^T \ 0 \ 0]^T. \end{aligned} \quad (21)$$

For $k \in [1, \dots, \infty]$, calculate the sigma points:

$$\mathcal{X}_{k-1}^a = [\hat{x}_{k-1}^a \ \hat{x}_{k-1}^a + \gamma\sqrt{P_{k-1}^a} \ \hat{x}_{k-1}^a - \gamma\sqrt{P_{k-1}^a}] \quad (22)$$

The UKF time-update equations are:

$$\begin{aligned} \mathcal{X}_{k|k-1}^x &= \mathbf{F}(\mathcal{X}_{k-1}^x, \ u_{k-1}, \ \mathcal{X}_{k-1}^\nu), \\ \hat{x}_k^- &= \sum_{i=0}^{2L} W_i^m \mathcal{X}_{i,k|k-1}^x, \\ P_k^- &= \sum_{i=0}^{2L} W_i^c (\mathcal{X}_{i,k|k-1}^x - \hat{x}_k^-)(\mathcal{X}_{i,k|k-1}^x - \hat{x}_k^-)^T, \\ \mathcal{Y}_{k|k-1} &= \mathbf{H}(\mathcal{X}_{k|k-1}^x, \ \mathcal{X}_{k-1}^n), \\ \hat{y}_k^- &= \sum_{i=0}^{2L} W_i^m \mathcal{Y}_{i,k|k-1} \end{aligned} \quad (23)$$

The UKF measurement-update equations are:

$$\begin{aligned} P_{\bar{y}_k \bar{y}_k} &= \sum_{i=0}^{2L} W_i^c (\mathcal{Y}_{i,k|k-1} - \hat{y}_k^-)(\mathcal{Y}_{i,k|k-1} - \hat{y}_k^-)^T, \\ P_{x_k y_k} &= \sum_{i=0}^{2L} W_i^c (\mathcal{X}_{i,k|k-1} - \hat{x}_k^-)(\mathcal{Y}_{i,k|k-1} - \hat{y}_k^-)^T, \\ \kappa_k &= P_{x_k y_k} P_{\bar{y}_k}^{-1} \bar{y}_k, \\ \hat{x}_k &= \hat{x}_k^- + \kappa_k (y_k - \hat{y}_k^-), \\ P_k &= P_k^- - \kappa_k P_{\bar{y}_k \bar{y}_k} \kappa_k^T \end{aligned} \quad (24)$$

where

$$\begin{aligned} x^a &= [x^T \ v^T \ n^T]^T, \\ \mathcal{X}^a &= [(\mathcal{X}^x)^T \ (\mathcal{X}^\nu)^T \ (\mathcal{X}^n)^T]^T, \text{ and} \\ \gamma &= \sqrt{L + \lambda} \end{aligned} \quad (25)$$

In addition, λ is the composite scaling parameter, L is the dimension of the augmented state, R^v is the process-noise covariance, R^n is the measurement-noise covariance, and W_i are the weights.

B. Controller reconfiguration

Controller re-design can be considered by model matching. As the nominal closed-loop system is known, the model of this system can be used as a description of the dynamical properties that the new controller should produce in connected with the faulty plant. That is, the closed loop system should match with the model of nominal loop. The nominal closed loop system is composed of the linear nominal plant.

$$\begin{aligned} x(k+1) &= Ax(k) + Bu(k) \\ y(k) &= Cx(k) \end{aligned} \quad (26)$$

and a state-feedback controller $u(k) = -\mathbf{K}x(k)$ both of which yield the model of the closed-loop system

$$\begin{aligned} \dot{x}(k) &= (A - B\mathbf{K})x(k) \\ y(k) &= Cx(k) \end{aligned} \quad (27)$$

If the controller does not use all the inputs u_f of the input vector u , the matrix \mathbf{K} has zero rows. When the fault f occurs, the faulty plant is given by:

$$\begin{aligned} x(k+1) &= A_f x(k) + B_f u(k) \\ y(k) &= C_f x(k) \end{aligned} \quad (28)$$

where the fault f has changed the system properties, which are now described by the matrices A_f , B_f and C_f . If the set of available inputs and outputs have changed, the matrices B_f and C_f having vanishing columns or rows, respectively. A new state feedback controller, $u(k) = -K_f x(k)$ should be found such that the closed-loop system

$$\begin{aligned} x(k+1) &= (A_f - B_f \mathbf{K}_f) x(k) \\ y(k) &= C_f x(k) \end{aligned} \quad (29)$$

behaves like the nominal loop. That is, the relation, $A - BK = A_f - B_f K_f$ has to hold, which means that both closed loop system have the similar dynamics. It cannot be satisfied, unless B and B_f have the same image, (like in the case of a redundant actuator). Therefore, the new controller K_f is chosen so as to minimize the difference:

$$\|(A - BK) - (A_f - B_f K_f)\| \quad (30)$$

The solution to this problem is given by:

$$\begin{aligned} K_f &= B_f^+ (A_f - A + BK) \\ &= (B_f' B_f)^{-1} B_f' (A_f - A + BK) \end{aligned} \quad (31)$$

where B_f^+ denotes the pseudo-inverse of B_f . The new controller is adapted to the faulty system and minimizes the difference between the dynamical properties of the nominal loop and the closed loop system with the faulty plant. In the proposed scheme, this has been done with the help of overlapping decomposition information set and model predictive control.

B.1 Model predictive control

Model predictive control (MPC) is a multi-variable control algorithm that solves, at each sampling instant, a finite horizon optimal control problem, and this involves an internal dynamic model of the process using receding horizon control, model assumptions and an optimization cost function J over the receding prediction horizon to calculate the optimum control moves.

• *Receding horizon control:* The MPC scheme makes use of the receding horizon principle. At each sample, a finite horizon optimal control problem is solved over a fixed interval of time, the prediction horizon. We assume that the controlled variables, $z(k)$, is to follow some set point trajectory, $r(k)$. A common choice is to use a quadratic cost function, which in combination with a linear system model yields a finite horizon linear quadratic problem. We assume that a model on the form:

$$\begin{aligned} x(k+1) &= Ax(k) + Bu(k), \\ y(k) &= C_y x(k), \\ z(k) &= C_z x(k) + D_z u(k), \\ z_c(k) &= C_c x(k) + D_c u(k) \end{aligned} \quad (32)$$

is available. Here $y(k) \in R^{p_y}$ is the measured output, $z(k) \in R^{p_z}$ the controlled output and $u(k) \in R^m$ the input vector. The state vector is $x(k) \in R^n$. The MPC controller should also respect constraints on control variables as well as the constrained outputs, $z_c(k) \in R^{p_c}$.

$$\begin{aligned} \Delta u_{min} &\leq \Delta u(k) \leq \Delta u_{max}, \\ u_{min} &\leq u(k) \leq u_{max}, \quad z_{min} \leq z_c(k) \leq z_{max} \end{aligned} \quad (33)$$

where $\Delta u(k) = u(k) - u(k-1)$ are the control increments. The distinction between controlled and constrained variables is natural, since only the controlled variables have specified reference values.

• *An optimal control problem:* The optimal control problem that is the core element of the MPC algorithm. Consider the following quadratic cost function:

$$\begin{aligned} J(k) &= \sum_{i=H_w}^{H_p+H_w+1} \|\hat{z}(k+i|k) - r(k+i|k)\|_Q^2 \\ &+ \sum_{i=0}^{H_u-1} \|\Delta \hat{u}(k+i|k)\|_R^2 \\ &- r(k+i|k)\|_R^2 \end{aligned} \quad (34)$$

where $\hat{z}(k+i|k)$ are the predicted controlled outputs at time k and $\Delta \hat{u}(k+i|k)$ are the predicted control increments. The matrices $Q \geq 0$ and $R > 0$ are weighting matrices, which are assumed to be constant over the prediction horizon. The length of the prediction horizon is H_p , and the first sample to be included

in the horizon is H_w . H_w may be used to shift the control horizon, but in the following presentation we will assume that $H_w = 0$. The control horizon is given by H_u . The cost function (34) may be rewritten as:

$$J(k) = \|Z(k) - \tau(k)\|_Q^2 + \|\Delta U\|_R^2 \quad (35)$$

where

$$Z(k) = \begin{bmatrix} \hat{z}(k|k) \\ \vdots \\ \hat{z}(k+H_p-1|k) \end{bmatrix}, \tau(k) = \begin{bmatrix} r(k|k) \\ \vdots \\ r(k+H_p-1|k) \end{bmatrix},$$

$$\Delta U(k) = \begin{bmatrix} \Delta u(k|k) \\ \vdots \\ \Delta u(k+H_u-1|k) \end{bmatrix},$$

$$Q = \text{diag}[Q \quad Q \quad \dots \quad Q], R = \text{diag}[R \quad R \quad \dots \quad R]$$

By deriving the prediction expressions, we can write

$$Z(k) = \Psi x(k) + \Gamma u(k-1) + \Theta \Delta U(k) \quad (36)$$

where

$$\Psi = \begin{bmatrix} C_z \\ C_z A \\ C_z A^2 \\ \vdots \\ C_z A^{H_p-1} \end{bmatrix}, \Gamma = \begin{bmatrix} D_z \\ C_z B + D_z \\ C_z A B + C_z B + D_z \\ \vdots \\ C_z \sum_{i=0}^{H_p-2} A^i B + D_z \end{bmatrix}$$

$$\Theta = \begin{bmatrix} D_z & 0 & \dots \\ C_z B + D_z & D_z & 0 \\ C_z A B + C_z B + D_z & \ddots & \vdots \\ \vdots & \ddots & 0 \\ C_z \sum_{i=0}^{H_p-2} A^i B + D_z & \dots & D_z \\ \vdots & \ddots & \vdots \\ C_z \sum_{i=0}^{H_p-2} A^i B + D_z & \dots & \dots \end{bmatrix}$$

Also, let

$$E(k) = \tau(k) - \Psi x(k) - \Gamma u(k-1) \quad (37)$$

This quantity could be interpreted as the free response of the system, if all the decision variables at $t = k$, $\Delta U(k)$, were set to zero.

Remark II.3: An efficient technique for interconnected systems is the overlapping decomposition [10]. The model predictive control has been derived here by subsystems from decentralized overlapping decomposition using the following steps. Consider the two systems.

$$\mathbf{S} : \dot{x} = Ax, \quad \tilde{\mathbf{S}} = \dot{\tilde{x}} = \tilde{A}\tilde{x} \quad (38)$$

where $x(t) \in \mathbf{R}^n$ is the state of \mathbf{S} and $\tilde{x}(t) \in \mathbf{R}^{\tilde{n}}$. According to the expansion-contraction or Inclusion Principle, $\tilde{\mathbf{S}}$ includes \mathbf{S} , or that \mathbf{S} is included by $\tilde{\mathbf{S}}$ iff

$$\tilde{x} = Vx, \quad \tilde{A} = VAU + M, \quad UV = I_n \quad (39)$$

It is obvious that the stability of $\tilde{\mathbf{S}}$ implies the stability of \mathbf{S} and further details about computing matrices U, V, M and other related issues can be found in.

Remark II.4: The problem of minimizing the cost function is a quadratic programming (QP) problem. The algorithm for obtaining the optimal control signal at each sample assumes that the present state vector is available. Since this is often not the case, state estimation is required. The celebrated separation principle, stating that the optimal control and optimal estimation problems solved independently, yields a globally optimal controller for linear systems, suggests an attractive approach. We let the solution of the optimization problem be based on an estimate of the state vector, $\hat{x}(k)$ instead of the true state vector $x(k)$. For this purpose, a Kalman filter can be used. Apart from estimating the state of the system, an estimator could be used to estimate disturbances, assuming that a disturbance model is available. For example, error-free tracking may be achieved by including a particular disturbance model in the observer.

Remark II.5: In our case of UKF-based fault detection (comprising of drift detection and parameter estimation), the following is constructed:

$$\hat{x}(k) = A\hat{x}(k) + g(u(k), y(k)) + B\hat{\xi}(k)f(u(k), y(k), \hat{x}(k)) + K(y(k) - \hat{y}(k)) \quad (40)$$

$$\hat{y}(k) = C\hat{x}(k) \quad (41)$$

where $\hat{x}(k) \in \mathbf{R}^n$ is the estimated vector and $\hat{\xi}(k)$ is an estimate of $\xi(k)$. The value of $\hat{\xi}(k)$ is set to ξ_H until a fault is detected. It is assumed that after a fault occurs, $\xi(k) = \xi_f = \text{constant} \neq \xi_H$, $|\xi_f| \leq \xi_0$. We introduce:

$$\begin{aligned} e_x(k) &= x(k) - \hat{x}(k), \\ e_y(k) &= y(k) - \hat{y}(k), \\ e_0(k) &= \xi_f - \hat{\xi}(k) \end{aligned} \quad (42)$$

Then, the reconfigurable fault control can be obtained that:

$$e_x(k+1) = (A - KC)e_x(k) + B[\xi_f f(u(k), y(k), x(k)) - \hat{\xi}(k)f(u(k), y(k), \hat{x}(k))], \quad (43)$$

$$e_y(k) = Ce_x(k) \quad (44)$$

The convergence of the above adaptive reconfiguration is guaranteed by the following theorem:

Theorem II.2: Under the assumption (II.1) and (II.2), the system (43) and following diagnostic algorithm.

$$\Delta\xi = \Gamma f^T(u(k), y(k), \hat{x}(k))Re_y(k) \quad (45)$$

can realize $\lim_{t \rightarrow \infty} e_x(k) = 0$ and a bounded $e_0(k) \in L^2$. Furthermore, $\lim_{k \rightarrow \infty} e_\xi(k) = 0$ under a persistent excitation, where R is given by (9), $\Gamma > 0$ is a weighting scalar.

Proof: Consider the following Lyapunov function

$$V(e(k)) = e_x^T(k)Pe_x(k) + \Gamma^{-1}e_\xi^2(k) \quad (46)$$

From (43) and (45), its first forward difference is:

$$\begin{aligned} \Delta V &= E\{V(e(k+1)|e_k, p_k)\} - V(e(k)) \\ &= E\{e^T(k+1)P_1e(k+1)\} - e^T(k)P_1e(k) \\ &= (A_e e_x + B_L u_e)^T P (A_e e_x + B_L u_e) - e_x^T(k)P e_x(k) \\ &= e^T(k)[(P(A - KC) + (A - KC)^T P) \end{aligned}$$

$$\begin{aligned} &+ PB[\xi_f f(u(k), y(k), x(k)) \\ &- \hat{\xi}(k)f(u\xi(k), y(k), \hat{x}(k))]e(k) \\ &- 2e_\xi(k)f^T(u(k), y(k), \hat{x}(k))Re_y(k) \end{aligned} \quad (47)$$

According to (II.1) and (II.2), one can further obtain that

$$\begin{aligned} \Delta V &\leq -e_x^T(k)Qe_x(k) - 2e_\xi(k)f^T(u(k), y(k), \hat{x}(k))Re_y(k) \\ &2e_x^T(k)C^T R\{e_\xi f(u(k), y(k), x(k)) - \\ &\hat{\xi}(k)f(u(k), y(k), \hat{x}(k))\} \end{aligned} \quad (48)$$

where $\rho_2 = \lambda_{\min}(Q) - 2\|C\| \cdot |R| \xi_0 L_0, |\xi_f| \leq \xi_0$, $Q > 0$ is chosen such that $\rho_2 > 0$. Inequality (48) implies the stability of the origin $e_x = 0$, $e_\xi = 0$ and the uniform boundedness of e_x and e_ξ with $e_x \in L_2$. On the other hand, from (43), \dot{e}_x is uniformly bounded as well. According to Barbalat's Lemma, one can get

$$\lim_{k \rightarrow \infty} e_x(k) = 0 \quad (49)$$

The persistent excitation condition means that there exist two positive constants σ and t_0 such that for all t the following inequality holds:

$$\begin{aligned} &\sum_{m=k}^{k+k_0} f^T(y(m), u(m), x(m))B^T B f^T(y(m), u(m), x(m)) \\ &\geq \sigma I. \end{aligned} \quad (50)$$

Then from (43), (45), (49) and (50), one can conclude that $\lim_{t \rightarrow \infty} e_\xi(k) = 0$. This completes the proof. ■

III. EVALUATION OF THE PROPOSED SCHEME

The evaluation of the proposed scheme has been made on the following systems:

- Interconnected CSTR units, and
- A quadruple tank system

The following sections show the detailed implementation and simulation of the proposed scheme.

A. Illustrative Example: Two Interconnected CSTR units

In this section, we introduce a benchmark example of a plant composed of interconnected units with recycle which has been used from [21]. A plant composed of two well-mixed, non-isothermal continuous stirred-tank reactors (CSTRs) with interconnections is considered, where three parallel irreversible elementary exothermic reactions of the form $A \xrightarrow{k_1} B$, $A \xrightarrow{k_2} U$, $A \xrightarrow{k_3} R$ take place. As shown in Fig. 2, the feed to CSTR 1 consists of two streams, one containing fresh A at flow rate F_0 , molar concentration C_{A0} and temperature T_0 , and another containing recycled A from the second reactor at flow rate F_R , molar concentration C_{A_2} and temperature T_2 . The feed to CSTR 2 consists of the output of CSTR 1, and an additional fresh stream feeding pure A at flow rate F_3 , molar concentration C_{A0_3} , and temperature T_{0_3} . The output of CSTR 2 is passed through a separator that removes the products and recycles unreacted A to CSTR 1. Due to the non-isothermal nature of the reactions, a jacket is used to remove/provide heat to both reactors. A leak in both flux may be simulated by means of the new coefficients

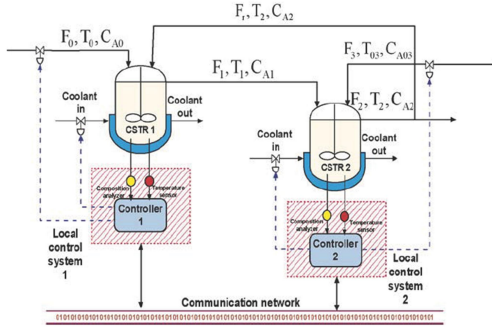


Fig. 2. Process flow diagram of two interconnected CSTR units.

α_1 and α_2 whose values are $0 < \alpha_1 \leq 1$ and $1 < \alpha_2 \leq 1$. The mathematical model of the faulty interconnected CSTR can be given as:

$$\begin{aligned} \dot{T}_1 &= \frac{\alpha_1 \times F_0}{V_1} (T_0 - T_1) + \frac{\alpha_1 \times F_R}{V_1} (T_2 - T_1) \\ &+ \sum_{i=1}^3 G_i(T_i) C_{A1} + \frac{Q_1}{\rho C_p V_1} \end{aligned} \quad (51)$$

$$\begin{aligned} \dot{C}_{A1} &= \frac{\alpha_1 \times F_R}{V_1} (C_{A0} - C_{A1}) + \frac{F_R}{V_1} (C_{A2} - C_{A1}) \\ &- \sum_{i=1}^3 R_i(T_i) C_{A1} V_1 \end{aligned} \quad (52)$$

$$\begin{aligned} \dot{T}_2 &= \frac{\alpha_2 \times F_1}{V_2} (T_1 - T_2) + \frac{\alpha_2 \times F_3}{V_2} (T_{03} - T_2) \\ &+ \sum_{i=1}^3 G_i(T_2) C_{A2} + \frac{Q_2}{\rho C_p V_2} \end{aligned} \quad (53)$$

$$\begin{aligned} \dot{C}_{A2} &= \frac{\alpha_2 \times F_1}{V_2} (C_{A1} - C_{A2}) + \frac{\alpha_2 \times F_3}{V_2} (C_{A03} - C_{A2}) \\ &- \sum_{i=1}^3 R_i(T_2) C_{A2} \end{aligned} \quad (54)$$

where $R_i(T_j) = k_{i0} \exp(-E_i/RT_j)$, $G_i(T_j) = (-\Delta H_i/\rho C_p)$ for $j = 1, 2$. ΔH_i , k_i , E_i , $i = 1, 2, 3$, denote the enthalpy, pre-exponential constants and activation energies of the three reactions, respectively. The control objective is to stabilize the plant at the (open-loop) unstable steady-state using the heat input rate Q_1 and the inlet reactant concentration C_{A0} as manipulated inputs for the first reactor, and using the heat input rate Q_2 and the inlet reactant concentration C_{A03} as manipulated inputs for the second reactor. Operation at the unstable point is typically sought to avoid high temperatures, while simultaneously achieving reasonable conversion. Under nominal conditions $\alpha_i = 1$, the performance may change suddenly or gradually when α_i is a function of time. The fault is modeled as a step function. The heat exchange surface has normally a transient degradation caused by the dirt on both sides of the wall.

B. Modeling of the quadruple tank system

The process is called quadruple-tank system and consists of four interconnected water tanks and two pumps. Its manipulated variables are voltages to the pumps and the controlled variables are the water levels in the two lower tanks. The quadruple-tank process is being built by considering the concept of two double-tank processes. The quadruple tank system presents a multi-input-multi-output (MIMO) system. This system is a real-life control problem prototyped to experiment on, and try to solve in the most efficient way, since it deals with multiple variables, thus it gives a reflection for the large systems in industry. The schematic description of the four tank system can be visualized by Figure 3. The system has two control inputs (pump throughputs) which can be manipulated to control the water level in the tanks. The two pumps are used to transfer water from a sump into four overhead tanks. By adjusting the bypass valves of the system, the proportion of the water pumped into different tanks can be changed to adjust the degree of interaction between the pump throughputs and the water levels. Thus each pump output goes to two tanks, one lower and another upper, diagonally opposite and the ratio of the split up is controlled by the position of the valve. Because of the large water distribution load, the pumps have been supplied 12 V each. The mathematical modeling of the quadruple tank process can be obtained by using Bernoulli's law. The constants are denoted in Table I. Combining all the equations for the interconnected four-tank system we obtain the physical system. A fault model can then be constructed by adding extra holes to each tank. The mathematical model of the faulty quadruple tank system can be given as (See equations (55)-(60)):

$$\begin{aligned} \frac{dh_1}{dt} &= -\frac{a_1}{A_1} \sqrt{2gh_1} + \frac{a_3}{A_1} \sqrt{2gh_3} \\ &+ \frac{\gamma_1 k_1}{A_1} \nu_1 + \frac{d}{A_1} - \frac{a_{leak1}}{A_1} \sqrt{2gh_1} \end{aligned} \quad (55)$$

$$\begin{aligned} \frac{dh_2}{dt} &= -\frac{a_2}{A_2} \sqrt{2gh_2} + \frac{a_4}{A_2} \sqrt{2gh_4} \\ &+ \frac{\gamma_2 k_2}{A_2} \nu_2 - \frac{d}{A_2} - \frac{a_{leak2}}{A_2} \sqrt{2gh_2} \end{aligned} \quad (56)$$

$$\begin{aligned} \frac{dh_3}{dt} &= -\frac{a_3}{A_3} \sqrt{2gh_3} + \frac{(1-\gamma_2)k_2}{A_3} \nu_2 \\ &- \frac{a_{leak3}}{A_3} \sqrt{2gh_3} \end{aligned} \quad (57)$$

$$\begin{aligned} \frac{dh_4}{dt} &= -\frac{a_4}{A_4} \sqrt{2gh_4} + \frac{(1-\gamma_1)k_1}{A_4} \nu_1 \\ &- \frac{a_{leak4}}{A_4} \sqrt{2gh_4} \end{aligned} \quad (58)$$

$$\frac{d\nu_1}{dt} = -\frac{\nu_1}{\tau_1} + \frac{1}{\tau_1} u_1 \quad (59)$$

$$\frac{d\nu_2}{dt} = -\frac{\nu_2}{\tau_2} + \frac{2}{\tau_2} u_2 \quad (60)$$

IV. SIMULATION RESULTS

In what follows, we present simulation results for the proposed fault tolerant scheme on two dynamical systems:

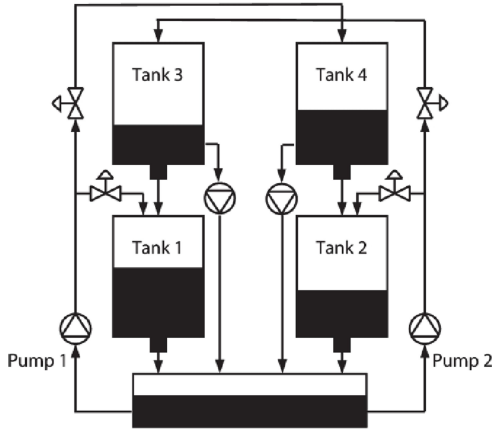


Fig. 3. Schematic diagram of a Quadruple tank system

- Interconnected CSTR units,
- Quadruple tank system.

A. Interconnected CSTR units

In what follows, we present simulation results for UKF for fault detection and then the fault tolerance with model predictive-based decentralized control. A series of simulation runs was conducted on the interconnected CSTR units to evaluate and the effectiveness of the proposed scheme based on the UKF fault detection and model-predictive-based decentralized fault control. To perform different set of experiment same fault scenarios have been used as defined. The details of the algorithm can be seen in [24].

A.1 Drift detection

A fault may occur in any phase or in any part of the plant. Critical faults not detected on time, can lead to adverse effects. In the sequel, the drift detection of the faults using UKF is clarified. It is seen from Fig. 4 that despite of an offset, the signature of fault is same to the nominal case. This is due to the closed-loop which is performing the job with a feedback, which may be also intrinsic in the physical mechanism of a real-time system generating the data, thus making the life difficult for fault detection, and suppressing the deviation and drifts. Thus, here, the UKF-based drift detection can give us a better picture for the fault scenario as shown in Fig. 5. The kinks seen in the middle of the flux leak profile of state 1 can alarm the engineer about some unusual practice going on in the process.

A.2 Information Fusion from UKF to Overlapping Decentralized Decomposition and MPC

Once, the parametric estimation is being done by the UKF, we are able to get system states for the leakage. For example, if we have flux leak in state 1, from UKF, the faulty state matrix can be extracted and fed into the MPC for appropriate control of faults. The results are being compared for the expanded version of the system control and the overlapping control, and it can be seen that the overlapping control is also performing its job

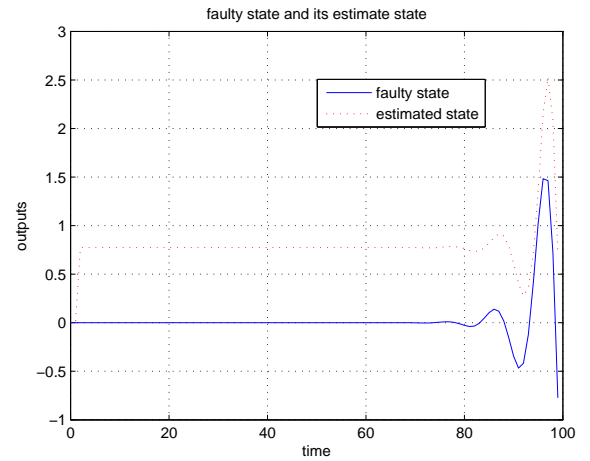


Fig. 4. Interconnected CSTR units: Leak Estimate and Fault Estimate of state 1

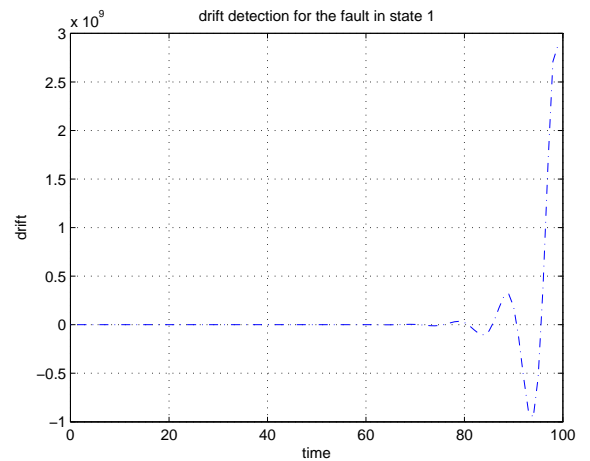


Fig. 5. Interconnected CSTR units: drift detection for the leak in state 1

by control the faults as can be seen in Figs. (6)-(9), which are giving a better response time towards the control of the system states, with less over-shoots and excitation.

Further, the information is fused in the model-predictive control, and the results show that the system somehow recovers itself from the faults rather than completely resulting in a breakdown of the system as can be seen in Fig. 10. This explains how with the help of unscented filter, the fault detection part is performed resulting in measuring the drift and parameter potency of fault in each state of CSTR, which then fed into in the information fusion, where with the help of overlapping decomposition and MPC, we are able to control the fault, given bounds of fault uncertainties.

B. Quadruple tank system

In what follows, we present simulation results for UKF for fault detection and then the fault tolerance with model predictive-based decentralized control. A series of simulation runs was conducted on the quadruple tank system to evaluate

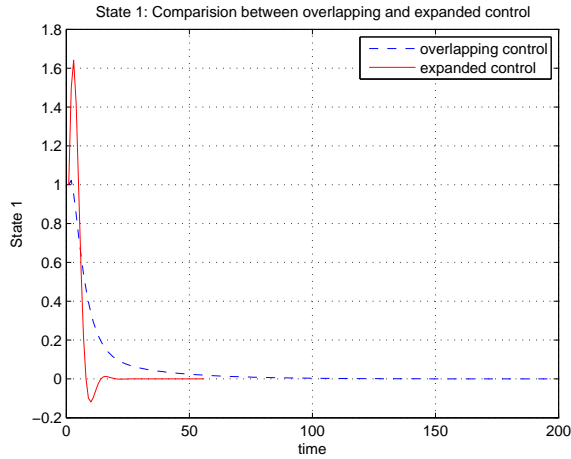


Fig. 6. Interconnected CSTR units State 1: Overlapping Decentralized Control

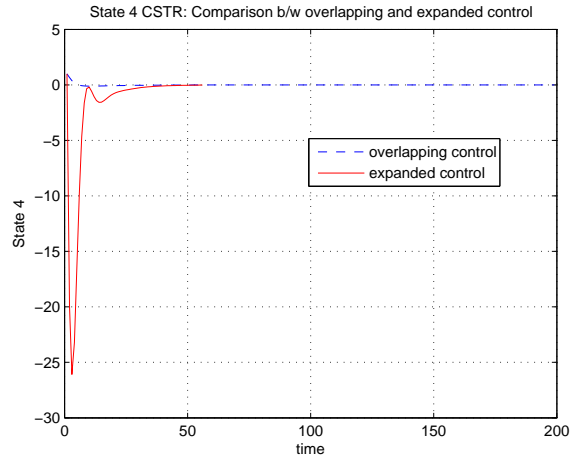


Fig. 9. Interconnected CSTR units State 4: Overlapping Decentralized Control

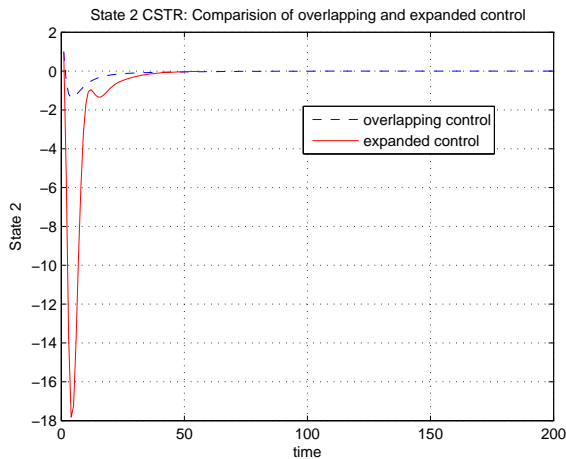


Fig. 7. Interconnected CSTR units State 2: Overlapping Decentralized Control

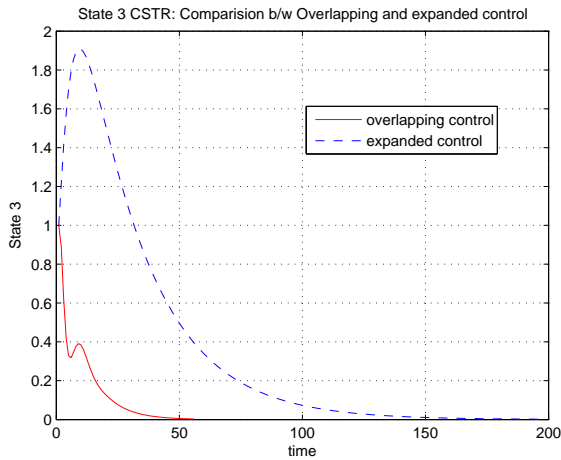


Fig. 8. Interconnected CSTR units State 3: Overlapping Decentralized Control

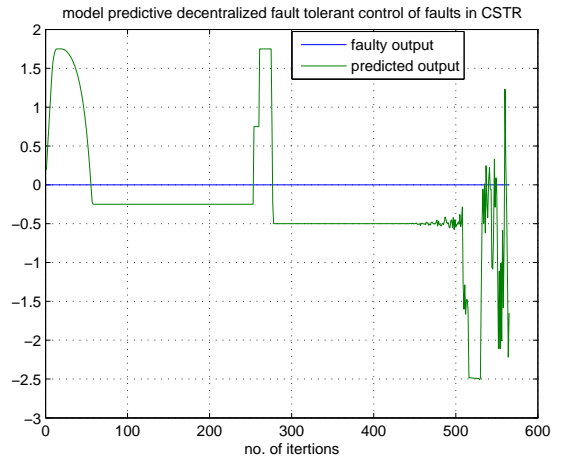


Fig. 10. Interconnected CSTR units: MPC-Based Decentralized Fault Tolerant Control

and the effectiveness of the proposed scheme based on the UKF fault detection and model-predictive-based decentralized fault control. To perform different set of experiment same fault scenarios have been used as defined.

B.1 Drift detection

A fault may occur in any phase or in any part of the plant. Critical faults not detected on time, can lead to adverse effects. In the sequel, the drift detection of the faults using UKF is clarified. It is seen from Fig. 11 that the fault is so incipient that apart from in the beginning, the level of water is achieving the same height. This is mainly due to the closed-loop system, where the controller is performing its job of achieving the desired set-point of water level in the tanks, thus suppressing any kind of deviations and drifts created due to leakage faults in particular. Considering this situation, UKF-based drift detection can give us a better picture for the fault scenario as shown in Fig. 12. The kinks shown in the middle of the height achievement of water in tank 1 can alarm the engineer about some unusual practice go-

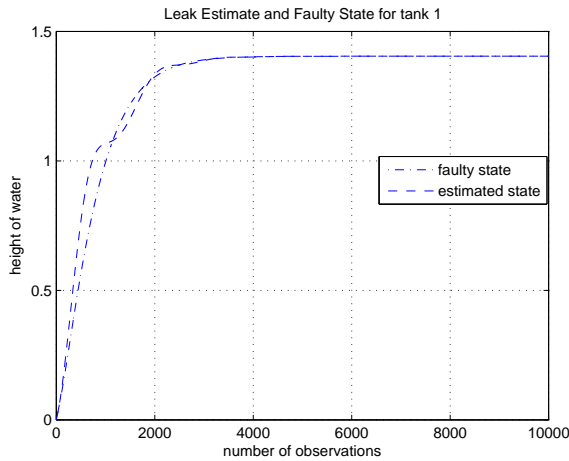


Fig. 11. Quadruple tank system: Leak Estimate and Fault Estimate of tank 1

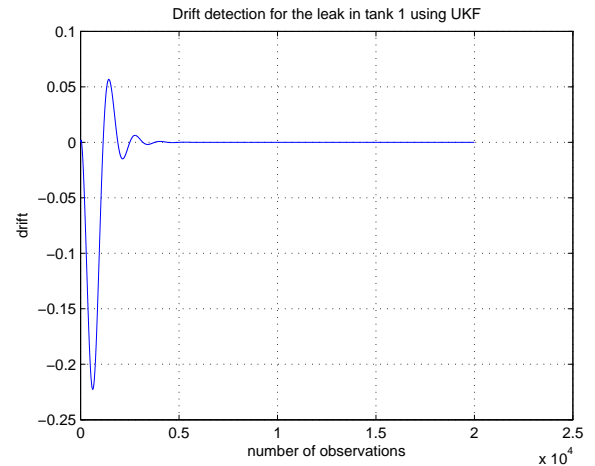


Fig. 12. Quadruple tank system: drift detection for the leak in tank 1

ing on in the process, thus preparing for some necessary action or constant monitoring.

B.2 Information Fusion from UKF to Overlapping Decentralized Decomposition and MPC

Once, the parametric estimation is being done by the UKF, we are able to get system states for the leakage fault. For example, if we have leakage in state 1, from UKF, the A matrix shown in (61) for the leakage is as follows:

$$A_{leak} = \begin{bmatrix} 1.0806 & 0.0034 & 0.0009 & -0.0877 \\ 1 & 0 & 0 & 0 \\ 0 & 1 & 0 & 0 \\ 0 & 0 & 1 & 0 \end{bmatrix} \quad (61)$$

This matrix is being fed into the model-predictive control algorithm in-order to upgrade it according to the fault at hand. The results are being compared for the expanded version of the system control and the overlapping control, and it can be seen that the overlapping control is also performing its job by controlling the faults as can be seen in Figs. (13)-(16) which are giving a better response time towards the control of the system states, with less over-shoots and excitation i.e. making it stable in less time. Further, the information is fused in the model-predictive control, and the results show that the system somehow recovers itself from the faults rather than completely result in a breakdown of the system as can be seen in Fig. 17. This explains how with the help of unscented filter, the fault detection part is performed resulting in measuring the drift and parameter potency of leakage fault in each tank state of QTS, which then fed into in the information fusion in the form of leakage matrix, where with the help of overlapping decomposition and MPC, we are able to achieve the desired set-point water-level of tank despite of leakage fault, given bounds of leakage fault.

V. CONCLUSION

In this paper, an effective integrated fault detection and fault tolerant control technique is developed for a class of interconnected process systems actuated by actuators and sensors that

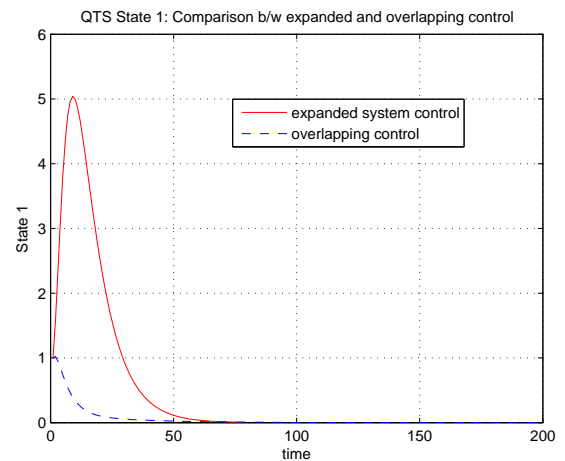


Fig. 13. Quadruple tank system State 1: Overlapping Decentralized Control

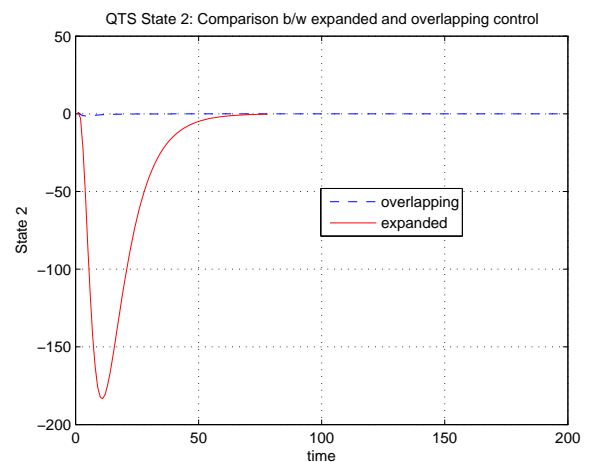


Fig. 14. Quadruple tank system State 2: Overlapping Decentralized Control

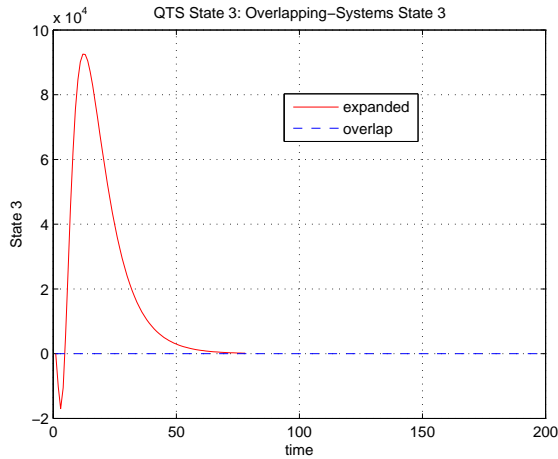


Fig. 15. Quadruple tank system State 3: Overlapping Decentralized Control

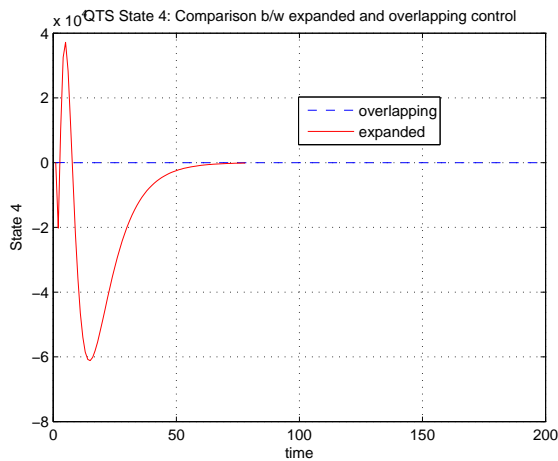


Fig. 16. Quadruple tank system State 4: Overlapping Decentralized Control

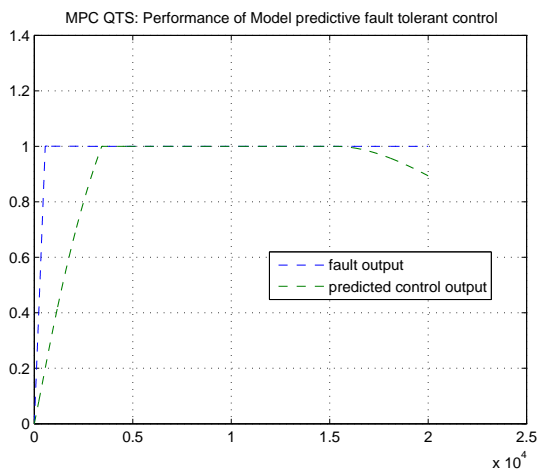


Fig. 17. Quadruple tank system: MPC-Based Decentralized Fault Tolerant Control

may undergo several different types of failures. Typical faults in interconnected process systems are considered next, and UKF based approach is being employed for fault detection and parameter estimation. The Fault detection system is then decentralized in that using overlapping decomposition technique. Model Prediction-based fault-tolerant controllers using the parameter estimates from the fault detection decentralized subsystem is designed next. It is demonstrated that all the signals in the system are bounded and that the tracking error converges to zero asymptotically despite multiple actuator and sensor faults. The proposed scheme has been successfully evaluated on interconnected CSTR units with recycle and quadruple tank system, thus underpinning the proposed scheme with its practical implementation.

ACKNOWLEDGMENTS

The authors would like to thank the reviewers for their The authors would like also to thank the deanship for scientific research (DSR) at KFUPM for support through research group project **RG-1105-1**.

REFERENCES

- [1] Parker, M. A., C. Ng, and L. Ran, 'Fault-Tolerant Control for a Modular Generator Converter Scheme for Direct-Drive Wind Turbines', *IEEE Trans. Industrial Electronics*, vol. 58, no. 1, pp. 305–315, 2011.
- [2] Dwari, S. and L. Parsa, 'Fault-Tolerant Control of Five-Phase Permanent-Magnet Motors With Trapezoidal Back EMF', *IEEE Trans. Industrial Electronics*, vol. 58, no. 2, pp. 476–485, 2011.
- [3] Sun, Z., J. Wang, G. W. Jewell and D. Howe, 'Enhanced Optimal Torque Control of Fault-Tolerant PM Machine under Flux-Weakening Operation' *IEEE Trans. Industrial Electronics*, vol. 57, no. 1, pp. 344–353, 2010.
- [4] de Lillo, L., L. Empringham, P. W. Wheeler, S. Khwan-On, C. Gerada, M. N. Othman and X. Huang, 'Multiphase Power Converter Drive for Fault-Tolerant Machine Development in Aerospace Application', *IEEE Trans. Industrial Electronics*, vol. 57, no. 2, pp. 575–583, 2010.
- [5] Zhao, W., K. T. Chau, M. Ji, Cheng, J. Zhu, 'Remedial Brushless AC Operation of Fault-Tolerant Doubly Salient Permanent-Magnet Motor Drives', *IEEE Trans. Industrial Electronics*, vol. 57, no. 6, pp. 2134–2141, 2010.
- [6] Ceballos, S., J. Pou, E. Robles, J. Zaragoza and J. L. Martin, 'Performance Evaluation of Fault-Tolerant Neutral-Point-Clamped Converters', *IEEE Trans. Industrial Electronics*, vol. 57, no. 8, pp. 2709–2718, 2010.
- [7] Siljak, D. D., 'Reliable Control using Multiple Control Systems', *Int. J. Control*, vol. 31(2), pp. 303–329, 1980.
- [8] Shimemura E. and M. Fujita 'A Design Method for Linear State Feedback Systems Processing Integrity Based on a Solution of a Riccati-Type Equation', *Int. J. Control*, vol. 42(4), pp. 887–899, 1985.
- [9] Zhao, Q., and J. Jiang, 'Reliable State Feedback Control Systems Design Against Actuator Failures', *Automatica*, vol. 34(10), 1267–1272, 1998.
- [10] Mahmoud, M. S., *Decentralized Control and Filtering in Interconnected Dynamical Systems*, CRC Press, Taylor and Francis Group, New York, 2010.
- [11] Chandler, P. R., 'Self-Repairing Flight Control System Reliability and Maintainability Program Executive Overview', *Proc. IEEE National Aerospace and Electronics Conference*, pp. 586590, 1984.
- [12] Moerder, D. D., N. Halyo, J. R. Broussard and A. K. Caglayan, 'Application of Precomputed Control Laws in a Reconfigurable Aircraft Flight Control System', *J. Guidance, Control, and Dynamics*, vol. 12(3), pp. 325–333, 1989.
- [13] Looze, D. P., J. L. Weiss, J. S. Eterno and N. M. Barrett, 'An Automatic Redesign Approach for Restructurable Control Systems', *IEEE Control Systems Magazine*, vol. 5, pp. 16–22, 1985.
- [14] Montoya, R. J., W. E. Howell, W. T. Bundick, A. J. Ostroff, R. M. Hueschen and C. M. Belcastro, 'Restructurable Controls', *Tech. Rep. NASA CP-2277*, Proc. of a Workshop held at NASA Langley Research Center, Hampton, VA, September 2122, 1982.
- [15] Monaco, J., D. Ward, R. Barron and R. Bird, 'Implementation and Flight Test Assessment of an Adaptive, Reconfigurable Flight Control System', *Proc. the 1997 AIAA Guidance, Navigation, and Control Conference*, pp. 1443–1454, 1997.

- [16] Maybeck, P. S. and R. D. Stevens, 'Reconfigurable flight control via multiple model adaptive control methods', *IEEE Trans. Aerospace and Electronic Systems*, vol. 27(3), pp. 470-479, 1991.
- [17] Rothenhagen, K. and F. W. Fuchs, 'Current Sensor Fault Detection, Isolation, and Reconfiguration for Doubly Fed Induction Generator', *IEEE Trans. Industrial Electronics*, vol. 56, no. 10, pp. 4239-4245, 2009.
- [18] E. A. Wan, R. V. der Merwe and A. T. Nelson, 'Dual estimation and the unscented transformation', in *Advances in Neural Information Processing Systems*, S. A. Solla, T. K. Leen, and K.R. Miller, Eds., Cambridge, MA: MIT Press, pp. 666-672, 2000.
- [19] Julier, S. J., J. K. Uhlmann, and H. Durrant-Whyte, 'A New Approach for Filtering Nonlinear Systems', *Proc. American Control Conference*, pp. 1628-1632, 1995.
- [20] Julier, S. J. and J. K. Uhlmann, 'A New Extension of the Kalman Filter to Nonlinear Systems', *Proc. Aero Sense: The 11th International Symposium on AeroSpace/Defense Sensing, Simulation and Controls*, vol. 3068, pp. 182-193, 1997.
- [21] Sun, Y. and N. H. El-Farra, 'Quasi-Decentralized Model-Based Networked Control of Process Systems', *Computers and Chemical Engineering*, vol. pp. 2016-2029, 2008.
- [22] Mogens B., M. Kinnaert, J. Lunze and M. Staroswiecki, *Diagnosis and Fault Tolerant Control*, 2nd Edition, Springer, 2006.
- [23] Noura, H., D. Theilliol, J.- C. Ponsart and A. Chamseddine, *Fault-Tolerant Control Systems: Design and Practical Applications*. Springer 2009.
- [24] M. S. Mahmoud and Haris M. Khalid, 'Fault Tolerant Scheme Detail Evaluation', *Internal Report, MsM-KFUPM-Tolerant-509*, 2010.
- [25] Xie X., Zhou D., Jin Y., 'Strong tracking filter based adaptive generic model control', *Journal of Process Control*, vol. 9, pp. 337-350, 1999.
- [26] Nazari, R., 'Fault-tolerant control of a magnetic levitation system using virtual-sensor-based reconfiguration', *2010 18th Mediterranean Conference on Control and Automation (MED)*, 23-25 June 2010, pp. 1067-1072.
- [27] Yetendje, A., 'Multisensor fusion fault-tolerant control of a magnetic levitation system', *2010 18th Mediterranean Conference on Control and Automation (MED)*, 23-25 June 2010, pp. 1055-1060.